INL/CON-08-14655
PREPRINT

Kinetic Modeling of a Fischer-Tropsch Reaction Over a Cobalt Catalyst in a Slurry Bubble Column Reactor for Incorporation into a Computational Multiphase Fluid Dynamics Model

2008 International Pittsburgh Coal Conference

Anastasia Gribik
Donna Guillen
Daniel Ginosar

September 2008

International Pittsburgh Coal Conference 2008
Pittsburgh, PA, USA
September 29 – October 2, 2008

KINETIC MODELING OF A FISCHER-TROPSCH REACTION OVER A COBALT CATALYST IN A SLURRY BUBBLE COLUMN REACTOR FOR INCORPORATION INTO A COMPUTATIONAL MULTIPHASE FLUID DYNAMICS MODEL

Anastasia Gribik, *Donna Guillen, PhD, PE, Daniel Ginosar, PhD*
Anastasia.Gribik@inl.gov, *Donna.Guillen@inl.gov, Daniel.Ginosar@inl.gov*
Idaho National Laboratory
PO Box 1625
Idaho Falls, ID 83415-3710

Abstract

Currently multi-tubular fixed bed reactors, fluidized bed reactors, and slurry bubble column reactors (SBCRs) are used in commercial Fischer Tropsch (FT) synthesis. There are a number of advantages of the SBCR compared to fixed and fluidized bed reactors. The main advantage of the SBCR is that temperature control and heat recovery are more easily achieved. The SBCR is a multiphase chemical reactor where a synthesis gas, comprised mainly of H_2 and CO, is bubbled through a liquid hydrocarbon wax containing solid catalyst particles to produce specialty chemicals, lubricants, or fuels. The FT synthesis reaction is the polymerization of methylene groups [-(CH_2)-] forming mainly linear alkanes and alkenes, ranging from methane to high molecular weight waxes.

The Idaho National Laboratory is developing a computational multiphase fluid dynamics (CMFD) model of the FT process in a SBCR. This paper discusses the incorporation of absorption and reaction kinetics into the current hydrodynamic model. A phased approach for incorporation of the reaction kinetics into a CMFD model is presented here. Initially, a simple kinetic model is coupled to the hydrodynamic model, with increasing levels of complexity added in stages.

The first phase of the model includes incorporation of the absorption of gas species from both large and small bubbles into the bulk liquid phase. The driving force for the gas across the gas liquid interface into the bulk liquid is dependent upon the interfacial gas concentration in both small and large bubbles. However, because it is difficult to measure the concentration at the gas-liquid interface, coefficients for convective mass transfer have been developed for the overall driving force between the bulk concentrations in the gas and liquid phases. It is assumed that there are no temperature effects from mass transfer of the gas phases to the bulk liquid phase, since there are only small amounts of dissolved gas in the liquid phase. The product from the incorporation of absorption is the steady state concentration profile of the absorbed gas species in the bulk liquid phase.

The second phase of the model incorporates a simplified macrokinetic model to the mass balance equation in the CMFD code. Initially, the model assumes that the catalyst particles are sufficiently small such that external and internal mass and heat transfer are not rate limiting. The model is developed utilizing the macrokinetic rate expression developed by Yates and Satterfield (1991). Initially, the model assumes that the only species formed other than water in the FT reaction is $C_{27}H_{56}$. Change in moles of the reacting species and the resulting temperature of the catalyst and fluid phases is solved simultaneously. The macrokinetic model is solved in conjunction with the species transport equations in a separate module which is incorporated into the CMFD code.

FT and SBCR Overview

Currently multi-tubular fixed bed reactors, fluidized bed reactors, and SBCRs are used in commercial FT synthesis. There are a number of advantages of the SBCR versus fixed and fluidized bed reactors. The main advantage of the SBCR is that temperature control and heat recovery are more easily achieved and mixing is enhanced (Fogler 1999). In SBCRs the reactant syngas, composed of H_2 and CO, is bubbled through a liquid hydrocarbon wax which contains the small, solid catalyst particles. Figure 1 presents a schematic of a SBCR identifying the various phases. The exothermic FT synthesis reaction is the polymerization of methylene groups [-(CH_2)-] forming mainly linear alkanes and alkenes, ranging from methane to high molecular weight waxes (Yates 1991):

$$n\mathrm{CO} + 2n\mathrm{H_2} \rightarrow -(\mathrm{CH_2})_n - + n\mathrm{H_2O} \qquad (1)$$

When an iron-based catalyst is used, water, one of the primary products of the FT reaction, can undergo a side reaction with CO to form CO_2 (water gas shift reaction):

$$\mathrm{H_2O} + \mathrm{CO} \rightarrow \mathrm{CO_2} + \mathrm{H_2} \qquad (2)$$

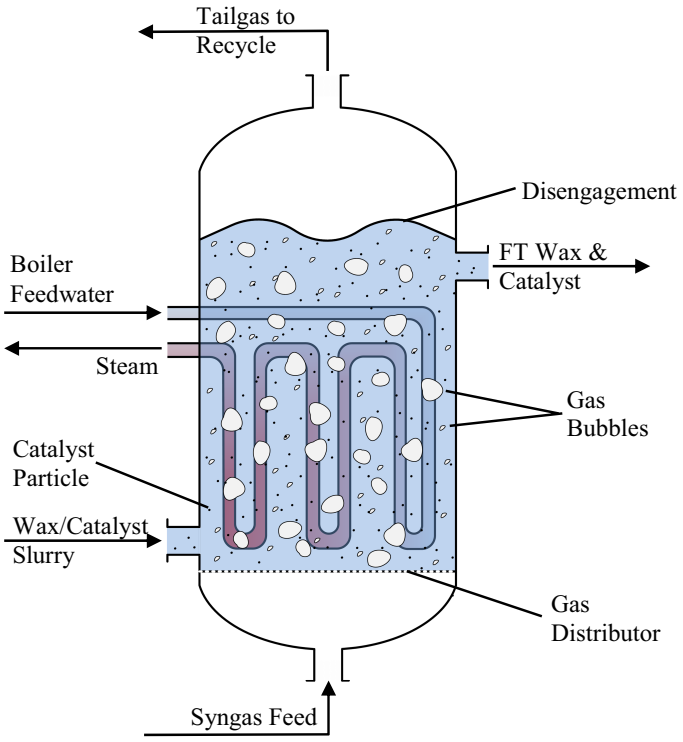

Figure 1. Schematic representation of a slurry bubble column reactor

Commercial catalysts for SBCRs are generally either cobalt or iron catalysts supported on titania (TiO_2), silica (SiO_2), or alumina (AlO_2). Iron based catalysts are less expensive than cobalt catalysts and are more selective for the production of olefins and light hydrocarbons. Iron catalysts also increase the activity of the water gas shift reaction and therefore produce larger amounts of oxygenates. Cobalt catalysts promote hydrogenation and deactivate less quickly than iron catalysts. Cobalt catalysts also do not promote the water gas shift reaction; therefore, there is little production of oxygenates (Maretto 1999). It should be noted that cobalt catalysts are more easily poisoned by sulfur contaminants than iron

catalysts; therefore, the syngas entering the reactor must have very low levels of sulfur compounds. For the initial model, polymerization is accomplished using a solid cobalt catalyst with an average particle size of 75 μm. This simplifies the model since the water gas shift reaction can be neglected. In future models, kinetic expressions for iron catalysts and the associated water gas shift reaction can be incorporated.

The following steps occur in the conversion of the gaseous reactants to products on a porous, supported catalyst (Bartholomew 2006):

1. Absorption from the gas phase reactants into the liquid phase across the bubble interface
2. Film mass transfer (bulk diffusion) of the reactants through the boundary layer surrounding the external surface of the solid catalyst particle (a boundary layer will exist if there is a relative velocity between the liquid and the catalyst)
3. Diffusion of reactants through the porous network of the catalyst to the catalytic surface
4. Adsorption of reactants onto the catalyst surface
5. Chemical reaction occurs at the catalytic sites on the catalyst surface
6. Desorption of the product from the catalytic surface
7. Diffusion of product through the porous network of the catalyst
8. Film mass transfer (bulk diffusion) of the product from the external surface of the solid catalyst particle through the boundary layer
9. Desorption of the gas phase products into the liquid phase across the bubble interface

Figure 2 depicts the concentration profile of the gas species involved in the FT reactions across the various interfaces.

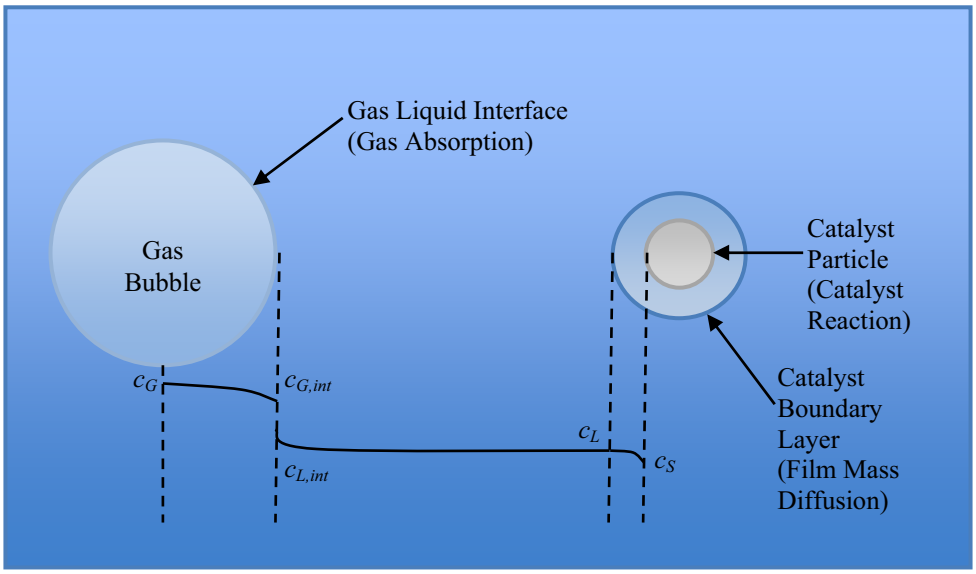

Figure 2. Concentration profile in the SBCR

Each of the steps listed above acts as a resistance to the overall reaction rate. An extensive literature search has been performed to assess the relative importance of the above reaction steps with respect to the overall reaction rate in the SBCR. From this search it has been determined that the limiting steps involve:

- Adsorption from the gas phase into the liquid phase
- Reaction of the absorbed gases with the catalyst

The following resistances have been neglected to simplify the overall rate expression:

1. Internal diffusion of the reactants in the porous catalyst can be neglected for the small catalysts used in current industrial FT reactors, i.e. for catalyst size ranges from 10 to 100 μm (Dry 2004). In addition, studies conducted by Post (1989) have found that reaction rates with iron and cobalt catalysts are only limited by intraparticle diffusion for catalyst particle diameters in excess of one millimeter. Therefore, the rate of intraparticle diffusion can be ignored for the catalyst in the proposed SBCR model.

2. The diffusion of the absorbed gases from the bulk liquid to the external surface of the solid catalyst can also be neglected. The resistance of mass transfer of the reactants from the bulk liquid to the catalyst particle is insignificant in comparison to that from the gas-bubble interface to the bulk liquid, since catalyst particle surface area is much greater than gas-bubble surface area (Satterfield 1980).

3. In addition, it is assumed that desorption and film mass transfer of the liquid product formed are not limiting.

Initially these phenomena are neglected to simplify the preliminary kinetic model. However, both intraparticle diffusion and mass transfer to the catalyst surface should be investigated after the initial simplified model is complete. Specifically, mass transfer will be investigated since the laminar layer formed around each catalyst particle is in a turbulent flow field, thereby providing a resistance for mass and heat transfer which may limit the rate of reaction. As a result, the temperature and the reactant concentrations on the catalyst surface can differ significantly from those in the bulk liquid.

The following sections outline the approaches for assessing the rates of gas absorption into the bulk liquid phase and the reaction kinetics associated with the catalyst surface reactions.

Absorption of Reactant Gas to Bulk Liquid Phase

The rate of absorption from the gas phase into the liquid phase is described by the governing equations for convective mass transfer between the two phases. This interphase transfer involves three transfer steps:

1. Mass transfer from the bulk gas phase to the gas side of the bubble interface

2. Mass transfer across the gas side of the bubble interface to the liquid side of the bubble interface

3. Mass transfer from the liquid side of the bubble interface to the bulk liquid phase

It is assumed that the rate of mass transfer between the two phases is controlled by the rates of diffusion through the phases on each side of the interface and no resistance is offered to the transfer of the diffusing

component across the interface. Since the gas is sparingly soluble[1] in the liquid phase, where gas-phase resistance is negligible, the material balance for the solute is based on the concentration gradient of the gas in the liquid phase. The driving force for the gas across the interface into the bulk liquid is dependent upon the interfacial concentration. However, because it is difficult to measure the concentration at the gas-liquid interface, coefficients for convective mass transfer across an interface have been developed for the overall driving force between the bulk concentrations in the gas and liquid phases. The following equation describes the rate of mass transfer (R_i [=] mol/m^{3}s) for the solute (gas) into the solvent (liquid):

$$R_i = k_L a_i \left(c_i^* - c_{i,L} \right) \tag{3}$$

with

$$c_i^* = \frac{c_{i,G}}{H_i} \tag{4}$$

where $k_L a_i$ is the overall mass transfer coefficient for species i (s^{-1}), c_i^* is the equilibrium concentration of species i in the gas phase with the liquid (mol/m^3), $c_{i,L}$ is the bulk concentration of species i in the liquid phase (mol/m^3), $c_{i,G}$ is the bulk concentration of species i in the gas phase (mol/m^3), and H_i is the Henry's constant for species i (Welty 2001). To simplify the model, it is initially assumed that only CO and H_2 is absorbed into the liquid phase. After the initial model is completed, additional gas species will be added to the adsorption model, including H_2O, CH_4, CO_2, C_2H_4, C_2H_6, and other light gas species.

The mass transfer coefficient ($k_L a_i$) will differ for the large and small bubbles. Previous studies have determined correlations for mass transfer coefficients for both large and small bubbles as a function of gas holdup and diffusivity (Maretto 1999):

$$\frac{k_L a_{i,large}}{\varepsilon_{G,large}} = 0.5 \sqrt{\frac{D_{L,i}}{D_{L,ref}}} \tag{5}$$

$$\frac{k_L a_{i,small}}{\varepsilon_{G,small}} = 1.0 \sqrt{\frac{D_{L,i}}{D_{L,ref}}} \tag{6}$$

where $\varepsilon_{G,large}$ is the gas holdup for large bubbles, $\varepsilon_{G,small}$ is the gas holdup for small bubbles $D_{L,i}$ are the diffusivities for species i in the liquid phase (m^2/s), and $D_{L,ref}$ is the reference diffusion coefficient in the liquid (m^2/s). Values for the diffusion coefficients, the reference diffusion coefficient, and the Henry's constant are presented in *Modeling of a Bubble Column Slurry Reactor for Fischer-Tropsch Synthesis* (Maretto 1999). However, efforts are underway to determine correlations for Henry's constants and diffusivities, as well as other physical properties, as a function of temperature for CO and H_2 in a variety of wax products, similar to commercially produced FT waxes. It is assumed that the absorption of the sparingly soluble gas into the liquid phase will not change the thermodynamic or physical properties of the liquid mixture significantly.

---

[1] The gas does not absorb significantly into the liquid phase; therefore, Henry's Law can be used to approximate the concentration of dissolved gas in the liquid. Henry's Law states that the amount of a given gas dissolved in a given type and volume of liquid is directly proportional to the partial pressure of the gas in equilibrium with the liquid.

Catalytic Surface Reaction Mechanisms

The kinetic model for the conversion of CO and H_2 on the catalyst surface can be modeled either as a macrokinetic or microkinetic model. Macrokinetic models provide simple rate expressions based on mechanistic models which have been fitted to rate data from kinetic studies for a range of reaction conditions. Macrokinetic models are limited to the range of reaction conditions they were fitted to; in addition, macrokinetic models should only be used for steady state models. For a detailed discussion on the limitation of macrokinetic models see *Fundamentals of Industrial Catalytic Processes* (Bartholomew 2006). Microkinetic models have the potential to address the problems associated with macrokinetic models using basic sets of elementary steps to derive rate expressions for all mechanisms associated with the chemical reaction. Despite significant progress in the development of microkinetic models for FT synthesis, this area of research is still nascent (Bartholomew 2006). Therefore, the initial kinetic model incorporated into the SBCR CMFD model is a macrokinetic model.

The initial model is developed utilizing the macrokinetic rate expression developed by Yates and Satterfield in 1991. The intrinsic kinetic expression for the consumption of CO and H_2, which is a Langmiur-Hinshelwood type expression, was based on data collected over a range of industrially relevant conditions. The reactor was a well-mixed, continuous flow, slurry reactor operated at temperatures of 200 to 240 °C, pressures of 0.5 to 1.5 MPa, and H_2 to CO feed ratios of 1.5 to 3.5 (Yates 1991).

$$-R_{CO} = \frac{a c_{CO,L} c_{H_2,L}}{\left(1 + b c_{CO,L}\right)^2} \tag{7}$$

$$-R_{H_2} = 2\left(-R_{CO}\right) \tag{8}$$

$$R_{H_2O} = -\left(-R_{CO}\right) \tag{9}$$

$$R_{-(CH_2)-} = -\left(-R_{CO}\right) \tag{10}$$

with the kinetic constant *a* and the adsorption coefficient *b* defined as follows (Yates 1991):

$$a = 8.852 \cdot 10^{-13} \exp\left[4494.41 \frac{1}{K}\left(\frac{1}{493.15} - \frac{1}{T}\right)\right] (R\,T)^2 \frac{m^6}{kg_{cat}\,s\,mol} \tag{11}$$

$$b = 2.226 \cdot 10^{-5} \exp\left[-8236.15 \frac{1}{K}\left(\frac{1}{493.15} - \frac{1}{T}\right)\right] R\,T \frac{m^3}{mol} \tag{12}$$

where R_{CO}, R_{H2}, R_{H2O}, and $R_{-(CH2)-}$ are the rates of consumption for CO and H_2 and the rate of production for H_2O and -(CH_2)-, respectively (mol/kg_{cat}s), *R* is the gas constant (J/mol-K), and *T* is the temperature of the catalyst (K). To get the rate of change in moles per volume the reaction rate, per mass of catalyst, the reaction rate is multiplied by the density of the catalyst and the corresponding catalyst volume fraction. It should be noted that the reaction expression above is only relevant for reactor temperatures close to the temperatures the rate expression was derived for. It is proposed that additional macrokinetic expressions be incorporated into the model to determine the effects of the kinetic rate expression on the rate of formation of hydrocarbons.

For the initial kinetic model, it is assumed that the hydrocarbon wax product formed can be approximated by $C_{27}H_{56}$. This is obviously a simplification of the range of products formed during the FT reaction,

which ranges from methane to hydrocarbons with carbon numbers into the hundreds. This assumption will affect the rheology of the liquid phase. Future refinements of the model will include calculating the specific mole fractions of the various hydrocarbons formed using the Anderson-Shulz-Flory (ASF) distribution. However, rather than using the traditional ASF distribution, a modified ASF distribution will be used to better match the actual performance of the FT catalyst for the specific chain growth probability factor (α). The product distribution for the traditional ASF distribution is as follows:

$$\ln x_n = \ln \frac{(1-\alpha)}{\alpha} + n \ln \alpha \qquad (13)$$

where x_n is the mass fraction with carbon number n. For this study it is assumed that α is equal to 0.92, which provides sufficiently large hydrocarbons for the production of synthetic diesel fuel (Bartholomew 2006). The following arbitrary correlation was used to shift the product distribution slightly toward increased production of liquid components:

$$x_n(Modified\,ASF) = x_n(Classical\,ASF) \times \left[1 - \alpha + 0.78^{\alpha}\right] \qquad (14)$$

An additional correction to the modified ASF distribution was used to better match the irregular distribution in the $C_1 - C_4$ product range. To accomplish this fit, the ASF correlation is not used for C_1 - C_4 products; rather, the mass fraction of the combined $C_1 - C_4$ products is calculated by difference as follows:

$$x_{C1-C4} = 1 - \sum_{n=5}^{\infty} x_n(Modified\,ASF) \qquad (15)$$

To obtain the individual distribution of $C_1 - C_4$ products, the following percentages of the total were assigned: 52% for C_1, 8% for C_2, 20% for C_3, and 20% for C_4. Figure 3 presents the performance of the classical and modified ASF distributions versus literature values for the actual product distribution (Bartholomew 2006).

It should be noted that the ASF distribution and the modifications described above only specify the carbon number, they do not differentiate between paraffins, olefins, or oxygenates of the same carbon number. Future refinements of the kinetic model should include calculation of the specific types of hydrocarbons formed. In addition, a correlation for α as a function of reactor conditions would improve the predictive capability of the model, specifically as a function of the temperature and pressure at the current reactor location.

For the initial model it is assumed that the slurry phase is well mixed. As a result the composition of the wax formed from the reaction of CO and H_2 on the catalyst surface immediately has the composition specified by a $C_{27}H_{56}$ hydrocarbon for the most simplistic case, or the composition specified by the modified ASF distribution. This is a reasonable assumption given that the SBCR operates in the churn turbulent region. Future refinements should include investigation into reaction rates for the actual polymerization reactions, i.e. a microkinetic model. This would allow investigation of the changes in wax species concentrations as a function of reactor location.

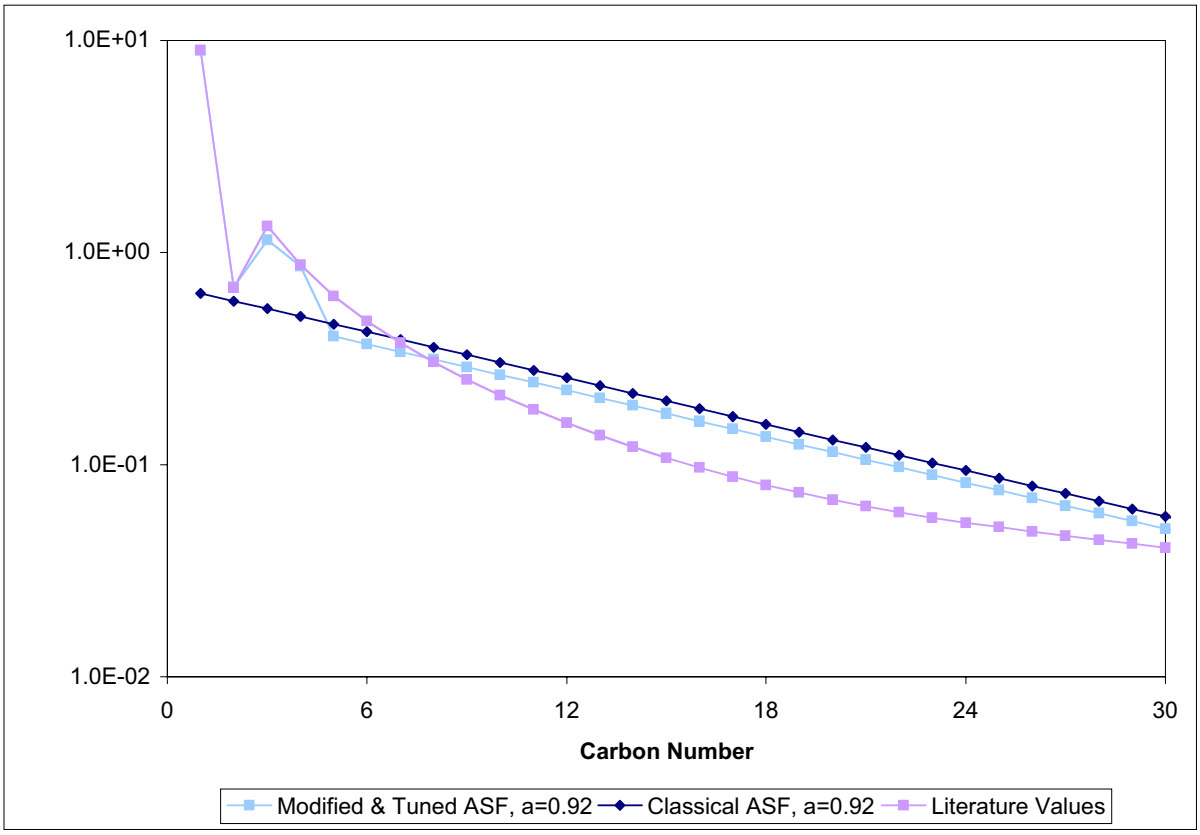

Figure 3. Performance of classical and modified ASF distribution versus measured product distribution

Kinetic Modeling Approach Summary

The absorption and kinetic models, specifically changes in species concentrations, are incorporated into the mass continuity equation in NPHASE. NPHASE is a computational multiphase fluid dynamics program for the prediction of multifield flows with mass, momentum, and energy transfer. Currently eight species are tracked in the SBCR model:

- CO in small bubbles, large bubbles, and the bulk fluid
- H_2 in small bubbles, large bubbles, and the bulk fluid
- $C_{27}H_{56}$ and H_2O in the bulk fluid

In addition, the model includes exothermic heating of the bulk fluid due to the exothermic FT reaction as well as heat removal from a constant temperature heat exchanger.

The first phase of the model includes incorporation of the absorption of gas species from both large and small bubbles into the bulk liquid phase. It was assumed that there were no temperature effects from the transfer of mass from the gas phases to the bulk liquid phase, since there are only small amounts of dissolved gas in the liquid phase because the gas is sparingly soluble in the bulk liquid. The product from the incorporation of absorption into NPHASE is the steady state concentration profile of absorbed gas species in the bulk liquid phase. Depending upon the hydrodynamics, there may be different regions

within the reactor with a higher concentration of large and/or small bubbles with a resultant effect on the concentration profile of the absorbed gas species.

The second phase of the model includes the addition of the simplified macrokinetic model to the mass balance equation in NPHASE. Again, the initial kinetic model assumes that the only species formed other than water in the FT reaction is $C_{27}H_{56}$. Change in moles of the reacting species and the resulting temperature of the catalyst and fluid phases due to the exothermic FT reaction are solved simultaneously with the transport equations for species *i* in each phase.

Once the initial simplified macrokinetic model is functional, the modified ASF distribution will be added to the kinetic model significantly increasing the complexity. In addition to incorporation of the modified ASF distribution, vapor liquid equilibrium (VLE) will be incorporated into the model. VLE will be calculated for the products formed in the FT reaction. Given the large range of products formed, it will be necessary to group the various alkanes formed into sets to maintain a reasonable computation time for the CMFD model. It is anticipated that five to ten sets of hydrocarbon groups will be incorporated into the model, not including C_1 to C_{10} which will be modeled as individual species.

The third phase of the model will include revisiting diffusion through the bulk liquid to the catalyst surface and intraparticle diffusion. The impact on the overall reaction rate will be assessed with the incorporation of the additional resistances to mass transfer in the system.

During the course of the project microkinetic models will be researched. If it is found that sufficiently detailed microkinetic models exist with the necessary supporting data, the approach of incorporating these models into NPHASE will be investigated. Figure 4 provides a graphical representation of the tasks for each phase. Table 1 lists the assumptions for each phase.

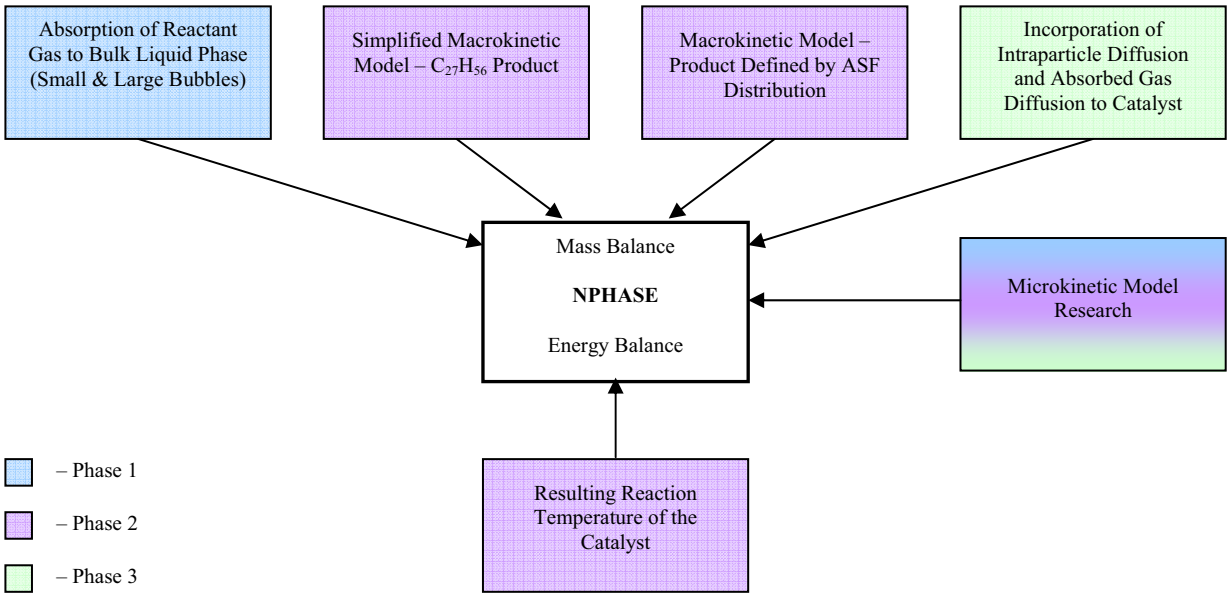

Figure 4. Kinetic model tasks and phases

Table 1. List of model assumptions and the corresponding basis for the assumption

Assumption	**Basis for Assumption**
Initial Model	
Neglect water gas shift reaction	Negligible for Co catalyst
Henry's Law can be used to approximate the concentration of dissolved gas in the liquid	CO and H_2 are sparingly soluble in the FT wax product
Wax-catalyst slurry is well mixed	Churn turbulent regime
Desorption and film mass transfer of the liquid product formed is not limiting	Reaction rate and gas absorption occur at a rate much slower than liquid-liquid mass transfer (well mixed assumption)
Phase 1 – Gas Absorption	
Model gas absorption into the liquid phase only, i.e. neglect kinetics	Simplification of the problem to ensure gas absorption is properly modeled
Phase 2 – Kinetic Incorporation	
Neglect pore diffusion	Negligible for particle < 1 mm diameter (Post 1989)
Neglect temperature gradients across the catalyst particle	Negligible for small catalyst particles (Iliuta 2007)
Neglect boundary layer around the catalyst particle	Catalyst-particle surface area is much greater than gas-bubble surface area (Satterfield 1980), also there is a small relative velocity difference between the liquid and catalyst
Phase 2a – Simplified Product	
Assume wax product is a homogeneous $C_{27}H_{56}$ mixture	Simplification of the kinetic model to ensure the kinetic model is functional
Phase 2b – Modified ASF Distribution	
Assume modified ASF Product distribution as well as incorporation of VLE into the model	Microkinetic models are still in research and development phase (Bartholomew 2006)
Phase 3 – Intraparticle Diffusion and Catalyst Boundary Layer	
Neglect temperature difference across catalyst boundary layer and catalyst particle	Negligible for small catalyst particles (Iliuta 2007)

Project Status

Currently, the first phase and a portion of the second phase of the kinetic model have been completed. A subroutine has been written which incorporates the gas phase absorption into the bulk liquid phase as well as the simplified macrokinetic model for the formation of $C_{27}H_{56}$ into the transport equations in the NPHASE code. The temperature effects on the gas, bulk liquid, and catalyst particles due to the exothermic heating of the FT reaction have also been incorporated. However, the physical properties for the gas and liquid species in the code have been approximated and are not a function of the reactor pressure and temperature. It is anticipated that physical property correlations for the simplified macrokinetic model with the formation of the $C_{27}H_{56}$ hydrocarbon will be incorporated into the model in the near future.

Nomenclature

ASF	Anderson-Shulz-Flory
CMFD	computational multiphase fluid dynamics
FT	Fischer Tropsch
SBCR	slurry bubble column reactors
VLE	vapor liquid equilibrium

$c_{i,G}$	mol/m^3	bulk concentration of species *i* in the gas phase
$c_{i,L}$	mol/m^3	bulk concentration of species *i* in the liquid phase
c_i^*	mol/m^3	equilibrium concentration of species *i* in the gas phase with the liquid
$D_{L,i}$	m^2/s	diffusivity for species *i* in the liquid phase
$D_{L,ref}$	m^2/s	reference diffusion coefficient in the liquid
H_i	unitless	Henry's constant for species *i*
k_La_i	s^{-1}	overall mass transfer coefficient for species *i*
n	unitless	carbon number
R	J/mol-K	gas constant
$R_{-(CH2)-}$	mol/kg$_{cat}$s	rate of production for -(CH_2)-
R_{CO}	mol/kg$_{cat}$s	rate of consumption for CO
R_{H2}	mol/kg$_{cat}$s	rate of consumption for H_2
R_{H2O},	mol/kg$_{cat}$s	rate of production for H_2O
R_i	mol/m^3	rate of mass transfer for the solute (gas) into the solvent (liquid)
T	K	temperature of the catalyst
x_n	unitless	mass fraction
α	unitless	chain growth probability factor
$\varepsilon_{G,large}$	unitless	gas holdup for large bubbles
$\varepsilon_{G,small}$	unitless	gas holdup for small bubbles

References

Bartholomew, C. H. and R. J. Farrauto, *Fundamentals of Industrial Catalytic Processes*, Second Edition, Hoboken: Wiley-Interscience, 2006, pp. 398 – 467.

Dry, Mark and André Steynberg, "Fischer-Tropsch Technology," *Studies in Surface Science and Catalysis*, Vol. 152, Amsterdam: Elsevier, 2004, pp. 533 – 566.

Fogler, H. Scott, *Elements of Chemical Reaction Engineering*, Third Edition, Upper Saddle River: Prentice Hall PTR, 1999, pp. 769-783.

Iliuta, I., et al, "Multicomponent Multicompartment Model for Fischer-Tropsch SCBR," *AIChE Journal*, Vol. 53, 2007, pp/ 2062-2083.

Knopf, F. C., et al, "Pulsing to Improve Bubble Column Performance: II. Jetting Gas Rates," *AIChE Journal*, Vol. 52, 2006, pp. 1621.

Maretto, C. and R. Krishna, "Modeling of a Bubble Column Slurry Reactor for Fischer-Tropsch Synthesis," *Catalysis Today*, Vol. 52, 1999, pp. 279-289.

Perry, Robert H. and Don W. Green, *Perry's Chemical Engineers' Handbook*, Eight Edition, New York: McGraw Hill, 2007, pp. 14-110 – 14-111.

Post, M. F. M., et al, "Diffusion Limitations in Fischer-Tropsch Catalysts," *AIChE Journal*, Vol. 35, 1989, pp. 1107-1114.

Satterfield, Charles N. and George A. Huff, "Effects of Mass Transfer on Fischer-Tropsch Synthesis in Slurry Reactors," *Chemical Engineering Science*, Vol. 35, 1980, pp. 195-202.

Welty, James R., et al, *Fundamentals of Momentum, Heat, and Mass Transfer*, Fourth Edition, New York: John Wiley & Sons, Inc., 2001, pp. 589 – 653.

Yates, Ian C. and Charles N. Satterfield, "Intrinsic Kinetics of the Fischer-Tropsch Synthesis on a Cobalt Catalyst," *Energy & Fuels*, Vol. 5, 1991, pp. 168-173.